Am J Cancer Res 2022;12(7):3333-3346
www.ajcr.us /ISSN:2156-6976/ajcr0143794

Original Article

Disulfiram blocked cell entry of SARS-CoV-2 via inhibiting the interaction of spike protein and ACE2

Hsiao-Fan Chen[1,8*], Po-Ren Hsueh[2*], Yen-Yi Liu[3*], Yeh Chen[4,7], Sui-Yuan Chang[5,6], Wei-Jan Wang[7,8], Chen-Shiou Wu[1,8], Ya-Min Tsai[5], Yu-Shu Liu[5], Wen-Chi Su[1,9], Yu-Chi Chou[10], Mien-Chie Hung[1,8,11]

[1]Graduate Institute of Biomedical Sciences, China Medical University, Taichung 406040, Taiwan; [2]Departments of Laboratory Medicine and Internal Medicine, China Medical University Hospital, School of Medicine, China Medical University, Taichung 404333, Taiwan; [3]Department of Public Health, College of Public Health, China Medical University, Taichung 406040, Taiwan; [4]Institute of New Drug Development, China Medical University, Taichung 406040, Taiwan; [5]Department of Clinical Laboratory Sciences and Medical Biotechnology, National Taiwan University College of Medicine, Taipei 100225, Taiwan; [6]Department of Laboratory Medicine, National Taiwan University Hospital and National Taiwan University College of Medicine, Taipei 100225, Taiwan; [7]Department of Biological Science and Technology, China Medical University, Taichung 406040, Taiwan; [8]Research Center for Cancer Biology, China Medical University, Taichung 406040, Taiwan; [9]Department of Medical Research, China Medical University Hospital, Taichung 404327, Taiwan; [10]Biomedical Translation Research Center (BioTReC), Academia Sinica, Taipei 115024, Taiwan; [11]Department of Biotechnology, Asia University, Taichung 41354, Taiwan. [*]Equal contributors.

Received April 28, 2022; Accepted June 25, 2022; Epub July 15, 2022; Published July 30, 2022

Abstract: Disulfiram is an FDA-approved drug that has been used to treat alcoholism and has demonstrated a wide range of anti-cancer, anti-bacterial, and anti-viral effects. In the global COVID-19 pandemic, there is an urgent need for effective therapeutics and vaccine development. According to recent studies, disulfiram can act as a potent SARS-CoV-2 replication inhibitor by targeting multiple SARS-CoV-2 non-structural proteins to inhibit viral polyprotein cleavage and RNA replication. Currently, disulfiram is under evaluation in phase II clinical trials to treat COVID-19. With more and more variants of the SARS-CoV-2 worldwide, it becomes critical to know whether disulfiram can also inhibit viral entry into host cells for various variants and replication inhibition. Here, molecular and cellular biology assays demonstrated that disulfiram could interrupt viral spike protein binding with its receptor ACE2. By using the viral pseudo-particles (Vpps) of SARS-CoV-2, disulfiram also showed the potent activity to block viral entry in a cell-based assay against Vpps of different SARS-CoV-2 variants. We further established a live virus model system to support the anti-viral entry activity of disulfiram with the SARS-CoV-2 virus. Molecular docking revealed how disulfiram hindered the binding between the ACE2 and wild-type or mutated spike proteins. Thus, our results indicate that disulfiram has the capability to block viral entry activity of different SARS-CoV-2 variants. Together with its known anti-replication of SARS-CoV-2, disulfiram may serve as an effective therapy against different SARS-CoV-2 variants.

Keywords: COVID-19, SARS-CoV-2 spike, ACE2, viral entry, drug repurposing

Introduction

In the 1930s, the workers in the rubber industry who used tetraethyl thiuram disulfide (TETD, disulfiram), an accelerator to stabilize rubber, subsequently developed an intolerance to alcohol [1]. Thus, it was considered as the treatment for alcohol dependency. In 1951, the FDA approved disulfiram (Antabuse®) as an alcohol-aversive agent to treat chronic alcoholism with well-established pharmacokinetics, safety, and tolerance [2]. Disulfiram inhibits acetaldehyde dehydrogenase and subsequently causes many highly unpleasant symptoms similar to a hangover, even with a small amount of alcohol consumption [3].

In addition to alcohol addiction, several studies investigated whether disulfiram could be a feasible anti-cancer therapeutic strategy [4, 5]. Studies have demonstrated that the anti-cancer effect of disulfiram is in a copper-dependent manner [6, 7]. Copper is an integral part of redox reactions and triggers reactive oxygen

species (ROS), essential molecules regulating inflammation and cancer progression [8]. Disulfiram forms a complex with copper that enhances ROS levels in promoting apoptosis of tumor cells via inhibition of NF-κB, a potent redox sensor and pro-survival factor [9]. Besides, the disulfiram-copper complex could induce autophagy-dependent apoptosis of cancer cells through induction of ER-stress and activation of the IRE1α-XBP1 pathway [10]. The disulfiram-copper complex could enhance PD-L1 expression, indicating that combination therapy with the disulfiram-copper complex and an anti-PD-1 antibody showed much better anti-tumor efficacy [11]. Several clinical trials have evaluated the anti-cancer efficacy of disulfiram-based therapies (https://www.cancer.gov/about-cancer/treatment/clinical-trials/intervention/disulfiram) [12, 13].

In addition to anti-tumor activity, disulfiram exhibited anti-bacterial [14, 15] and anti-parasitic properties [16, 17]. Interestingly, there are also studies to show disulfiram is associated with anti-viral activities. For example, there has been a clinical trial assessing its anti-viral potential in reactivating latent HIV-1 to deplete these viral reservoirs [18, 19]. disulfiram has been shown to act as a zinc-ejecting agent for the NS5A protein of the hepatitis C virus to inhibit HCV replication [20]. It also can inhibit papain-like proteases (PL^{pro}) of MERS and SARS coronavirus by targeting their Zn-bound cysteines [21]. The coronavirus disease 2019 (COVID-19), caused by severe acute respiratory syndrome coronavirus 2 (SARS-CoV-2), has been a global pandemic, resulting in massive socioeconomic hardship. In spite of global, far-reaching efforts, effective, cost-efficient, and safe drugs for COVID-19 are under intensive investigation and development. Since de novo anti-viral development has been notoriously lengthy and costly, a widely available, inexpensive drug that could be identified and repurposed against SARS-CoV-2 would be beneficial to current socioeconomic constraints. Most studies have chosen to target a single SARS-CoV-2 protein, including the spike protein that mediates cell entry, the main protease (M^{pro}), or PL^{pro} that cleaves the viral polyprotein into RNA-dependent RNA polymerase (RdRp), an essential enzyme for viral replication [22, 23]. Notably, Several studies suggested that disulfiram is able to target multiple non-structural proteins of SARS-CoV-2, such as M^{pro}, PL^{pro}, nsp10, nsp13 ATPase, and nsp14 exoribonuclease, and inhibit their enzyme activities leading to suppression of the viral polyprotein cleavage and RNA replication [24-26]. These studies indicate that disulfiram is a druggable, pharmacological molecule to target COVID-19.

Since its discovery in 2019, several novel variants of SARS-CoV-2 have appeared in multiple countries with combinations of mutations and deletions in the spike protein [27]. These mutations make these variants more powerful and infectious than the original SARS-CoV-2. Most of these variants contain different mutations in the receptor-binding domain (RBD) of spike protein. It appears that these mutations are responsible for increased viral infectivity, virulence, and immune evasion potency [34]. It will be the primary concern because these highly transmissible variants of SARS-CoV-2 are now surging worldwide [1]. Therefore, it is of great interest to determine the potency of disulfiram for its inhibitory activities on SARS-CoV-2 cell entry in various variants.

Materials and methods

FRET-based enzyme activity assay of M^{pro}

The FRET-based enzyme activity assay of M^{pro} was established in our previous study [28]. SARS-CoV-2 M^{pro} was incubated with different concentrations of disulfiram (1, 5, 10, 30, or 60 μM) in 20 mM Tris pH 8.0, 20 mM NaCl at room temperature for 30 mins. Fluorescent protein substrate CFP-YFP was added to initiate the reaction. The activity assay was measured for 30 mins by detecting the fluorescent signal at a wavelength of 474 nm after excitation at a wavelength of 434 nm. The reaction velocity was calculated using the data points from the first 15 mins and normalized to the DMSO control.

FRET-based enzyme activity assay of PL^{pro}

A 50 μl reaction mixture containing purified SARS-CoV-2 PL^{pro} and different concentrations of disulfiram (1, 5, 10, 30, or 60 μM) in assay buffer was pre-incubated at room temperature for 30 mins. Peptide substrate (Z-RLRGG-AMC, BACHEM) was then added to start the reaction. The fluorescence signal was monitored continuously at 30°C by detecting emis-

sion at a wavelength of 460 nm with excitation at a wavelength of 360 nm. The reaction velocity was calculated by using all the data points and normalized to the DMSO control.

ELISA assay for ACE2-spike protein interaction

The inhibitory effects of disulfiram on the interaction between SARS-CoV-2 spike protein and human ACE2 were measured by the SARS-CoV-2 ELISA Kit (AllBio). Briefly, horseradish peroxidase (HRP)-conjugate-ACE2 was pre-incubated with various concentrations of disulfiram (200, 100, 50 μM) at room temperature for 30 mins, followed by addition to the ELISA plate pre-coated with SARS-CoV-2 spike RBD at 37°C for 1 hour. Each well was aspirated and then was washed with washing buffer five times. After the last wash, 90 μl TMB (3,3,5,5-Tetramethylbenzidine, AllBio) substrate solution was added to each well and incubated at 37°C for 20 mins. The color development was then stopped by adding a 50 μl Stop solution, and the HRP activity was measured by detecting the optical density at 450 nm. The binding rate or interaction between SARS-CoV-2 spike RBD and human ACE2 was calculated using the following equation: Spike-ACE2 interaction (%) is the ratio of averaged OD450 values of the sample/DMSO control × 100%.

FRET-based enzyme activity assay for TMPRSS2

The purification of catalytic domain of human TMPRSS2 protein was established in our previous study [29]. The reaction mixture containing TMPRSS2 protein and different concentrations of disulfiram (50, 100, or 200 μM) in 25 mM Tris pH 8.0, 150 mM NaCl was pre-incubated at room temperature for 30 mins. The Boc-Gln-Ala-Arg-AMC substrate (BACHEM) was then added to initiate the reaction. The fluorescence signal was continuously monitored at an emission wavelength of 440 nm with excitation at 340 nm. The reaction velocity was calculated by using all the data points and normalized to the DMSO control.

Cell culture

The VeroE6 cell line (African green monkey kidney cells) was grown in Dulbecco's Modified Eagle's Medium (DMEM, Gibco, USA) supplemented with 10% fetal bovine serum (FBS, Gibco, USA), 1 × GlutaMAX (Gibco, USA), and 1% penicillin/streptomycin (P/S, Hyclone, USA). The Calu3 cell line (human lung cancer cells) was preserved in Modified Eagle's Medium (MEM, Gibco, USA) supplemented with 10% FBS and 1% P/S. VeroE6 and Calu3 cells with stable expression of TMPRSS2 were generated by transfection with the pCMV3-TMPRSS2-Flag plasmid (Sino Biology) and selection by 400 μg/ml hygromycin. The human embryonic kidney cells 293T stably expressing recombinant human ACE2 (293T-ACE2) were generated by transfection with the pCMV3-ACE2 plasmid (Sino Biology) and maintained in DMEM containing 10% FBS, 1% P/S, and 200 μg/μl hygromycin. All these cells were cultured at 37°C and 5% CO_2.

Viral pseudo-particle infection assay

All SARS-CoV-2-Spike viral pseudo-particles were purchased from the RNAi core of the Academia Sinica, Taiwan (http://rnai.genmed.sinica.edu.tw/), and they were generated based on the VSV packaging system with spike protein of wild-type and different variants and luciferase reporter gene. Briefly, cells were seeded into 96-well plates and pretreated with different doses of disulfiram for 1 hour, then inoculated with 50 μl pseudovirions (0.1 MOI, multiplicity of infection). After incubation for one day, cell viability was confirmed by the Cell Counting Kit-8 (CCK-8) assay (Dojindo Laboratories, Japan). Each sample was mixed with 100 μl luciferase substrate (Bright-Glo Luciferase Assay System, purchased from Promega, USA), and luminescence was measured immediately by the GloMax Navigator System (Promega, USA). Viability-normalized relative light unit (RLU) was set as 100% for the control group, and the relative infection rate of the treated groups was calculated. All experiments were performed in triplicates and repeated three times independently.

Cytotoxicity assay

The cytotoxicity of disulfiram was assessed by seeding cells in 96 well plates in 100 μl media and cultured for 24 hours, followed by treatment with different doses of disulfiram in 50 μl complete medium containing for another 24 hours. The medium was removed, and viable cells were detected with MTT assay (Cyrusbioscience, Taiwan), which was read by absor-

bance at 570 nm by an ELISA reader. All experiments were performed independently in triplicates and repeated three times.

Viruses

Sputum specimens obtained from SARS-CoV-2-infected patients were maintained in viral transport medium. Virus in the specimens was propagated in VeroE6 cells in Dulbecco's modified Eagle's medium (DMEM) supplemented with 2 μg/mL tosylsulfonyl phenylalanyl chloromethyl ketone (TPCK)-trypsin (T1426, Sigma-Aldrich, USA). Culture supernatant was harvested when cytopathic effect (CPE) was observed in more than 70% of cells, and the virus titer was determined by plaque assay. The virus isolates used in the current study were hCoV-19/Taiwan/NTU13/2020 (GISAID: EPI_ISL_422415), hCoV-19/Taiwan/NTU49/2021 (GISAID: EPI_ISL_1010718) and hCoV-19/Taiwan/NTU92/2021 (EPI_ISL_3979387). The virus isolation was conducted in the Biosafety Level-3 Laboratory at National Taiwan University Hospital. The study was approved by the NTUH Research Ethics Committee (202101064RINB), and the participants gave written informed consent.

Plaque assay

Plaque reduction assay was performed in triplicate in 24-well tissue culture plates. SARS-CoV-2 (100-200 plaque forming unit, pfu/well) was incubated with test compounds for 1 h at 37°C before adding to the cell monolayer for another one hour. Subsequently, mixtures of virus and test compounds were removed and the cell monolayer was washed once with PBS before covering with media containing 1% methylcellulose for 5-7 days. The cells were fixed with 10% formaldehyde overnight. After removal of overlay media, the cells were stained with 0.5% crystal violet and the plaques were counted. The percentage of inhibition was calculated as [1 - (VD/VC)] × 100%, where VD and VC refer to the virus titer in the presence and absence of the test compound, respectively. DMSO was used to prepare serial dilution of test compounds and was used as the solvent control.

Yield reduction asasay

The VeroE6 cells were seeded to the 24-well culture plate at 2×10^5 cells/well in DMEM with 10% FBS and penicillin G sodium 100 units/mL, streptomycin sulfate 100 μg/mL and amphotericin B 250 ng/mL (antibiotic-antimycotic, Gibco, USA) one day before infection. The virus (0.02 MOI) was pre-mixed with the test compound at indicated concentrations, solvent control or medium containing 2% FBS (E2) for 1 hour at 37°C. After that, the mixture was added to the cells for another one hour of incubation at 37°C. At the end of incubation, the virus inoculum was removed and the cells were washed once with PBS buffer before adding fresh E2 medium (500 μL/well) containing test compound at indicated concentrations or solvent control for 24 hours at 37°C. Finally, the cellular RNA was extracted by NucleoSpin RNA Kit (Macherey-Nagel GmbH&Co. KG, Germany) for real time PCR analysis of SARS-CoV-2 E genes using the iTaq Universal Probes One-Step RT-PCR Kit (Bio-Rad, USA) and the QuantStudio™ 5 Real-Time PCR System (Applied Biosystems™, USA). All of the experiments involving SARS-CoV-2 virus were performed in the Biosafety Level-3 Laboratory of the First Core Laboratory, National Taiwan University College of Medicine.

Molecular docking

The RBD-ACE2 complex (PDB ID: 6VW1) was used as the template structure for the docking experiment. All the modeling processes were performed on (PS)2v3 structure prediction service [30]. Initially, we used the RBD sequence of the Wuhan-Hu-1 isolate (NC_045512.2) to replace the RBD sequence of 6VW1 to generate our wild-type (WT) docking target using (PS)2V3 protein structure prediction server [31]. The B.1.1.7 docking target was made by mutating the N501 to Y501. Only the residues around the RBD-ACE2 interaction surface were selected for the docking purpose. The B.1.351 target was established by introducing N501Y, E484K and K417N mutations into the WT target. L452R and T478K, and K417T, E484K and N501Y were introduced to generate B.1.617.2 and P1 variants. The docking target of current major spreading variant, B.1.1.529 was also modeled by making G339D, S371L, S373P, S375F, K417N, N440K, G446S, S477N, T478K, E484A, Q493R, G496S, Q498R, N501Y, Y505H mutations. Docking tasks were performed for WT and all variants using iGEMDOCK [32] with "GA Parameters" setting of Population size= 300, Generation=80, and Number of soluti-

ons=100. The best docking pose (solution) with the smallest docking score was selected for further representation. On the other hand, The frequency distribution of the docking scores of 100 docking poses found for the WT, B.1.1.7, B.1.351, B.1.617.2, P1 and B.1.1.529 targets are depicted. All the docking results visualization was represented using the PyMOL Molecular Graphics System, Version 2.0 Schrödinger, LL.

Results

Disulfiram interrupts the interaction of spike and ACE2

Previous studies indicated that disulfiram significantly inhibited the enzymatic activity of SARS-CoV-2 M^{pro} and PL^{pro} [24, 25]. Hence, we confirmed that with a fluorescence resonance energy transfer (FRET) assay to evaluate the inhibitory activity of disulfiram on the enzymatic activity of M^{pro} and PL^{pro} of SARS-CoV-2 [28, 33]. The IC50 of disulfiram against M^{pro} or PL^{pro} was 2.45 μM and 13.06 μM, respectively (Supplementary Figure 1A, 1B), supporting that disulfiram is able to inhibit enzyme activity for SARS-CoV-2 replication. It is not yet clear whether disulfiram has the capacity to block the efficiency of SAR-CoV-2 to enter host cells. Since numerous studies on the cell entry mechanisms of SARS-CoV-2 indicated that SARS-CoV-2 uses both human ACE2 as an entry receptor and human protease TMPRSS2 as an entry activator [34], we performed ELISA assays to measure the effect of disulfiram on the interaction of ACE2-spike protein, and FRET assays for the enzymatic activity of TMPRSS2. As shown in **Figure 1A**, we found that disulfiram blocked the interaction in a dose-dependent manner, yet interestingly, it did not affect the TMPRSS2 activity (**Figure 1B**). Thus, these results suggested that disulfiram may associate with an activity to inhibit viral entry of SARS-CoV-2 through interruption of the interaction of ACE2-spike protein in addition to the known mechanism, which blocks SARS-CoV-2 replication.

Disulfiram inhibited SARS-CoV-2 vpp infection, independent of TMPRSS2, furin, or copper-dependent pathway

To further investigate the potential activity of disulfiram to inhibit SARS-CoV-2 viral entry, a SARS-CoV-2 viral pseudo-particles (vpp) infection assay was performed (**Figure 1C**). First, we assessed three cell lines: 293T-ACE2, VeroE6, and Calu3. Intriguingly, the results showed that disulfiram treatment significantly inhibited the entry of SARS-CoV-2 vpp in a dose-dependent manner in different cell models (**Figure 1D**). VeroE6 cells originating from African green monkey kidney are commonly used for in vitro studies of the SARS-CoV-like viruses. Previous studies have shown that the TMPRSS2-expressing VeroE6 cell line is highly susceptible to SARS-CoV-2 infection [35]. Calu3 cells originating from human airway epithelium are served as TMPRSS2-positive cells. SARS-CoV-2 entry into these cells is dependent on TMPRSS2 [36]. In addition to TMPRSS2, furin, another host protease, has been identified to be responsible for S protein cleavage during virus entry [37, 38]. The inhibitory effect of disulfiram against SARS-CoV-2 vpp was not enhanced in the TMPRSS2-expressing cells or furin expressing cells (Supplementary Figure 2A-C), suggesting that disulfiram may not go through the TMPRSS2 or furin pathway to inhibit SARS-CoV-2 vpp infection. Moreover, studies have shown that the disulfiram and copper combination greatly enhances its antitumor efficacy [7]. Thus, we examined whether a combination of copper with disulfiram could increase the inhibitory effects against cell entry of SARS-CoV-2 vpp. As shown in Supplementary Figure 2D, the copper supplement did not enhance the inhibitory activity of disulfiram. In conclusion, our results suggested that disulfiram could inhibit cell entry of SARS-CoV-2 vpp likely by blocking the interaction of ACE2 and spike protein, but not through TMPRSS2, furin, or copper-dependent pathway.

Disulfiram blocks SARS-CoV-2 wild type and the other variants viral pseudo-particles infection

Next, we asked whether disulfiram could prevent vpps carrying different mutant forms of spike protein from infecting host cells. To this end, we performed the vpp infection assay with wild-type and five different variant vpps, including B.1.1.7 (known as the alpha variant, initially discovered in the UK), B.1.351 (beta variant, in South Africa), P1 (gamma variant, in Brazil), B.1.617.2 (delta variant, in India), and B.1.1.529 (omicron variant, in South Africa).

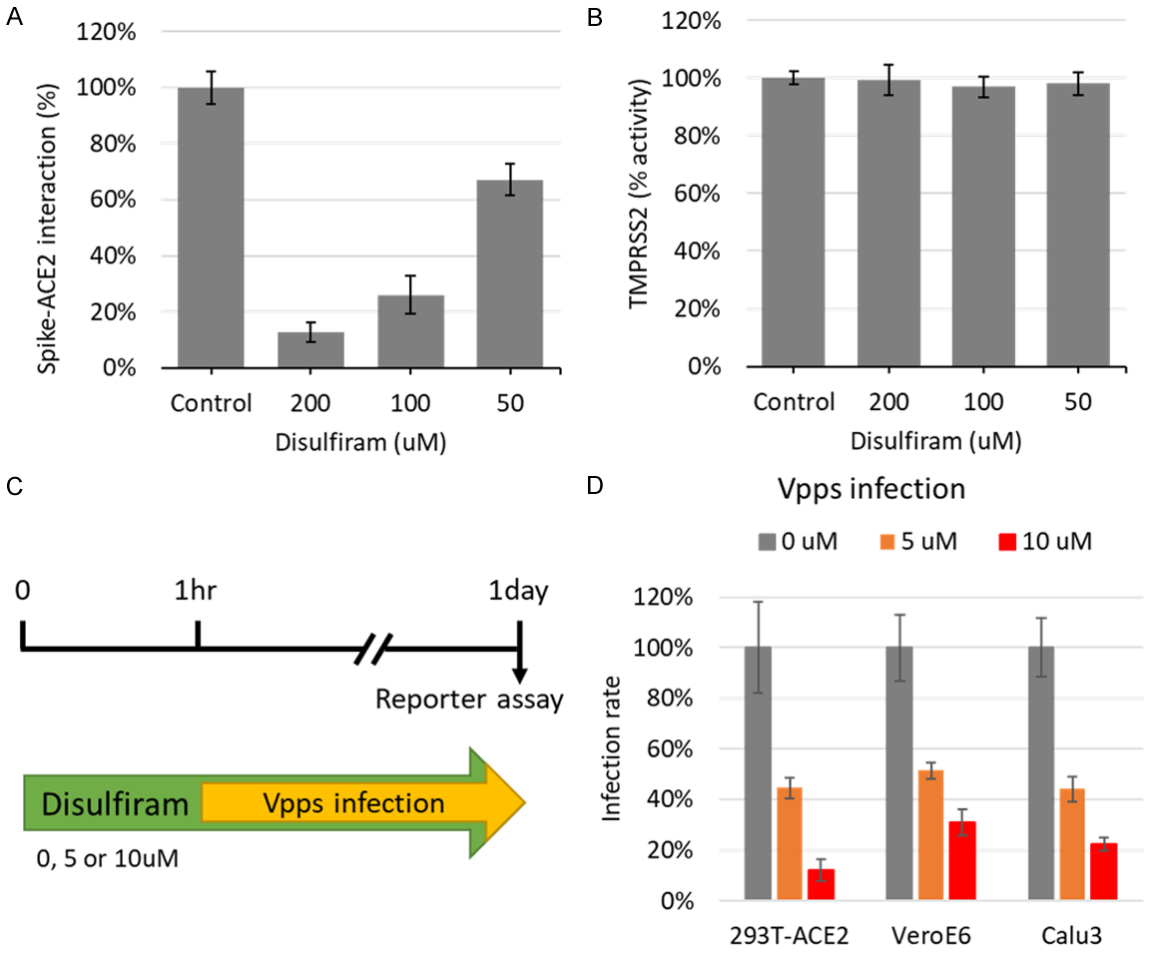

Figure 1. Disulfiram, an FDA-approved drug, blocked the Spike-ACE2 interaction and SARS-CoV-2 viral pseudo-particles infection and was independent of TMPRSS2. A. The percentage of Spike-ACE2 interaction from ELISA-base assay was shown with increasing amounts of disulfiram. B. The TMPRSS2 enzymatic activity was measured by using a FRET-base assay with the indicated concentration of disulfiram. C. Schematic illustrating method of SARS-CoV-2 spike viral pseudo-particles (Vpps) infection assay was shown. Cells were treated with disulfiram and Vpps as depicted and then collected for reporter assay after one day. D. The infection rate of SARS-CoV-2 wild-type spike Vpps was shown in the 293T-ACE2, VeroE6, or Calu3 cells with 5 μM or 10 μM disulfiram treatment. All data are shown as mean ± SD (n=3).

The results showed that disulfiram inhibited different variants of vpp infection in a dose-dependent manner in 293T-ACE2 (**Figure 2A**) and VeroE6 cells (**Figure 2B**). To further evaluate the activity of disulfiram, the inhibitory effects (EC50) on the vpp infection were measured in both cell lines (**Figure 2E**, **2F**). The cytotoxic effects (CC50) of disulfiram were also evaluated (**Figure 2C-F**). The selectivity index [SI] is determined by CC50/EC50 ratio. The ideal drug should have a relatively low toxic concentration but a high active concentration. An SI value lower than 2 indicates either low selectivity or general toxicity, whereas the values higher than 2 exhibit selectivity [39]. Generally, the compound which had an SI value >10 was assumed to belong to a great candidate for future drug development [40]. The highest SI values of disulfiram have occurred for wild-type vpp infection in 293T-ACE2 cells (SI=13.17) and VeroE6 cells (SI=5.05). Otherwise, the SI values of disulfiram for variant vpp infection are slightly lower than the wild-type vpp but still higher than 4 (**Figure 2E**, **2F**). These results suggested that disulfiram retains its inhibitory effect on vpp entry activity from different SARS-CoV-2 variants tested.

Disulfiram is able to suppress SARS-CoV-2 virus infection through inhibiting viral entry

We found that disulfiram could prevent viral entry in cell-based assays by vpps infection

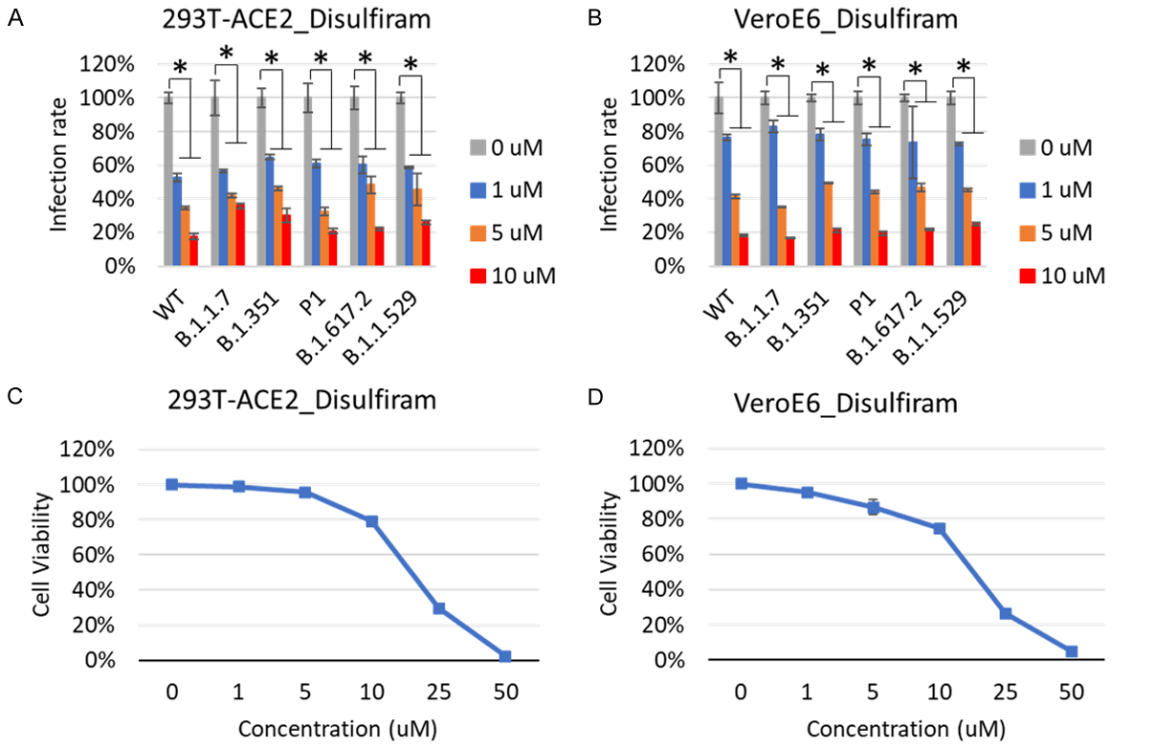

E

293T-ACE2_ Disulfiram	CC50 (uM)	EC50 (uM)	SI (CC50/IC50)
Wild type	17.25	1.31	13.17
B.1.1.7	17.25	1.98	8.71
B.1.351	17.25	3.03	5.69
P1	17.25	1.81	9.53
B.1.617.2	17.25	2.37	7.27
B.1.1.529	17.25	2.23	7.74

F

VeroE6_ Disulfiram	CC50 (uM)	EC50 (uM)	SI (CC50/IC50)
Wild type	15.65	3.10	5.05
B.1.1.7	15.65	3.18	4.92
B.1.351	15.65	3.84	4.08
P1	15.65	3.23	4.85
B.1.617.2	15.65	3.45	4.54
B.1.1.529	15.65	3.38	4.63

Figure 2. Disulfiram blocked SARS-CoV-2 wild type and the other variant vpps infection. A and B. 293T-ACE2 and VeroE6 cells were pretreated with varying concentrations of disulfiram for one hour and infected with SARS-CoV-2 spike Vpps of different variants. After 24 hours of infection, the infection efficiency rate was measured according to luciferase activities. The *P* values are indicated by stars, *P<0.05. C and D. 293T-ACE2 and VeroE6 cells were treated with indicated concentrations of disulfiram, and cell viability was detected by MTT assay. E. and F. The CC50 and EC50 of disulfiram were determined by using GraphPad PRISM software. CC50/EC50 measured the selective index (SI). All data are shown as mean ± SD (n=3).

assay. Next, we ask if it could also be observed in the live virus assay. A previous report demonstrated that the disulfiram against infection of SARS-CoV-2 live virus using immunofluorescence assay to detect SARS-CoV-2 N protein expression [25]. Similarly, we observed the inhibitory effects of disulfiram on viral infection against B.1.1.7 variants using a plaque assay (Supplementary Figure 3), supporting the results from the vpps assay (**Figure 2**). However, inhibition of disulfiram against live virus infection could be attributed to blocking viral entry and/or replication. To examine the anti-viral entry activity of disulfiram, we design the virus yield reduction assay with two treatment models (**Figure 3A**).

In the post-treatment model, cells were treated with varying concentrations of disulfiram for one day after the virus was incubated with host

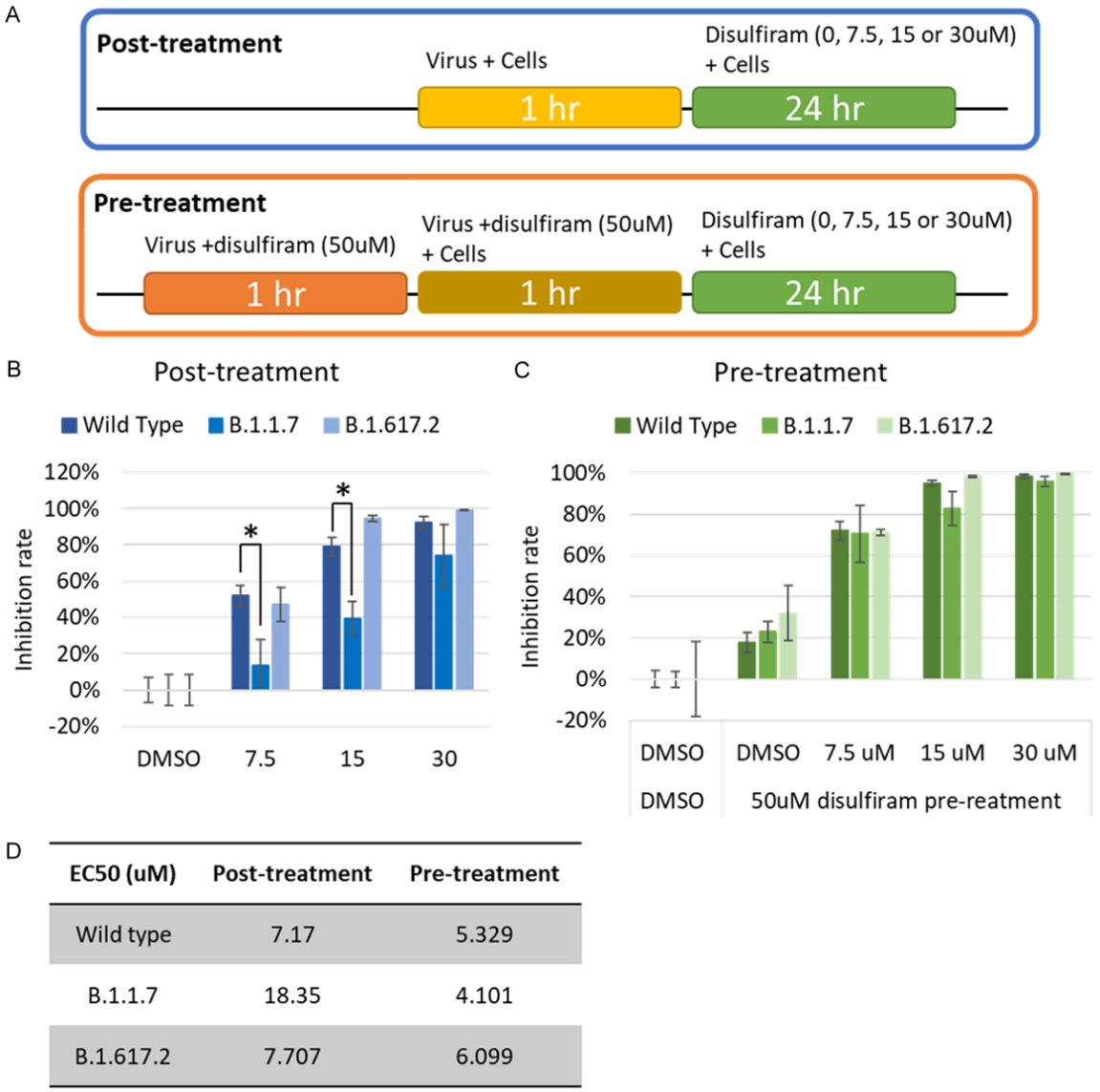

D

EC50 (uM)	Post-treatment	Pre-treatment
Wild type	7.17	5.329
B.1.1.7	18.35	4.101
B.1.617.2	7.707	6.099

Figure 3. Disulfiram repressed SARS-CoV-2 virus infection. A. The schematic illustrates two methods of disulfiram treatment of VeroE6 cells infected with the SARS-CoV-2 virus. In the post-treatment model, cells were treated with different concentrations of disulfiram after virus infection. In the pre-treatment model, viruses were pre-mixed 50 μM disulfiram for one hour before incubation with cells. Cells were continuously treated with different concentrations of disulfiram after infection with the disulfiram and virus mixture for another 1 hour. B. The inhibition rate of disulfiram against the SARS-CoV-2 wild-type, B.1.1.7 or B.1.617.2 variant was normalized with DMSO control in the post-treatment model. Data are shown to represent mean ± SD (N=3). The *P* values are indicated by stars, *P<0.05. C. The inhibition rate of 50 μM disulfiram pre-treatment and following different concentrations of disulfiram treatment against SARS-CoV-2 wild-type virus, B.1.1.7 or B.1.617.2 variant was normalized with DMSO control. Data are shown to represent mean ± SD (N=3). D. The EC50 of disulfiram from panels B and C was determined using GraphPad PRISM software.

cells for one hour then washed away through medium changes three times. Quantitative reverse transcription-polymerase chain reaction (RT-qPCR) was performed to evaluate the inhibition of virus infection on supernatants. The results showed that the disulfiram significantly repressed the yield of viral RNA in a dose-dependent manner after wild-type, B.1.1.7 or B.1.617.2 variants infection (**Figure 3B**). Because the cells were treated with disulfiram after the virus was infected and removed from the medium, the inhibitory effect of disulfiram would mainly be attributed to inhibiting viral replication. The EC50 value of disulfiram against

the B.1.1.7 variant virus was higher than that of the wild-type virus in the post-treatment group (**Figure 3D**). Besides, the EC50 value of disulfiram against the B.1.617.2 variant virus was similar to wild-type virus in the post-treatment group (**Figure 3D**). These results indicated that disulfiram treatment after infection had a less inhibitory effect against B.1.1.7 virus, which could be due to either the B.1.1.7 variant enhancing viral entry activity to host cells during the one hour infection period or increasing resistance to drug treatment (e.g., enhanced replication efficiency) during the one-day incubation period [41, 42].

Next, we performed the pre-treatment model to understand the importance of disulfiram on inhibiting viral entry. In the pre-treatment group, viruses were pre-mixed with 50 μM disulfiram for 1 hour; the disulfiram and virus mixture were incubated with cells for another 1 hour to allow interaction among disulfiram, viruses, and host cells. After the pre-treatment step, the virus and disulfiram were washed away with PBS buffer to stop the activity for virus to enter host cells; then, the cells were incubated without (**Figure 3C**) or with (**Figure 3D**) different concentrations of disulfiram for one day. The supernatants were collected to measure the inhibition of virus infection by RT-qPCR. We also perform a MTT assay to ensure 50 μM disulfiram pre-treatment do not affect the cell viablility (Supplementary Figure 4). Interestingly, we observed that the inhibition rate of one-hour pre-treatment with the 50 μM disulfiram and following DMSO control treatment 24 hours yields about 20% inhibition for both wild-type virus and B.1.1.7 variant and 30% inhibition for the B.1.617.2 without disulfiram for the one day incubation (**Figure 3C**). Since after the one hour exposure to disulfiram, the virus and drug in the medium were washed away, then the cells were incubated with medium only without disulfiram. The results indicated that the 20-30% inhibition mainly came from the one hour exposure resulting from inhibition of viral entry. The results also indicated no significant difference for disulfiram to inhibit viral entry between the wild-type, B.1.1.7, and B.1.617.2 variants (**Figure 2**). In addition, Compared to the post-treatment group, the EC50 value of disulfiram against wild-type, B.1.1.7 variant and B.1.617.2 variant virus was decreased in the pre-treatment group (**Figure 3C**, **3D**), this lower EC50 value is due to the pre-treatment of the disulfiram causing approximately 20-30% less virus when exposed to different concentration of drugs. In conclusion, these results indicated that disulfiram was able to inhibit the viral entry of SARS-CoV-2 for wild-type virus, B.1.1.7 and B.1.617.2 variant with similar potency. It also suggested that disulfiram could significantly reduce viral replication processes with less potency for B.1.1.7. variant. Furthermore, such dual inhibition activities of disulfiram might enhance the potency of disulfiram to inhibit the SARS-CoV-2, B.1.1.7 and B.1.617.2 variants infection.

Disulfiram docking analysis for wild type and variants of SARS-CoV-2

Disulfiram can block SARS-CoV-2 infection based on interrupting the interaction of ACE2 and spike proteins (**Figure 1A**). To understand how disulfiram would interfere and prevent the binding between the ACE2 and wild-type or different spike mutants, we analyzed one hundred docking poses of disulfiram for the targets of wild-type (WT), B.1.1.7, B.1.351, P1, B.1.617.2, and B.1.1.529 variants of SARS-CoV-2_RDB-hACE2 complex. Two docking pose was found for wild-type, but only one docking pose for B.1.1.7, B.1.351, P1, B.1.617.2, and B.1.1.529 variants each. The stability of docking disulfiram to B.1.1.7 and B.1.1.529 (DG1) are similar, and docking stability among B.1.617.2, B.1.351, and P1 (DG2) are also similar. The rank of the stability for docking disulfiram is DG2>DG1>WT (**Figure 4A**). The side-chain conformations of all variant's RDB residues change compared to the WT's, but the location of disulfiram was similar between these different variants (**Figure 4B**). Meanwhile, the docked poses of disulfiram are similar among wild-type, B.1.351 and P1 (Pose 1), and between B.1.1.7 and B.1.1.529 (Pose 2). The disulfiram docked pose for B.1.1.617.2 (Pose 3) is very different from Pose 1 and Pose 2 (Supplementary Figure 5). The environment of the binding pockets of wild-type and the other variants with disulfiram are mainly hydrophobic (**Figure 4C**). The binding affinity of disulfiram predicted by using PRODIGI platform [43] for WT is -5.2 kcal/mol, -5.2 kcal/mol for B.1.1.7, -5.1 kcal/mol for B.1.351, -5.1 kcal/mol for P1, -5.1 kcal/mol for B.1.617.2-5.0 kcal/mol and for B.1.1.529. In conclusion, the results of docking analysis suggested that disulfiram had comparable activity to prevent wild type or the other variant binding to ACE2

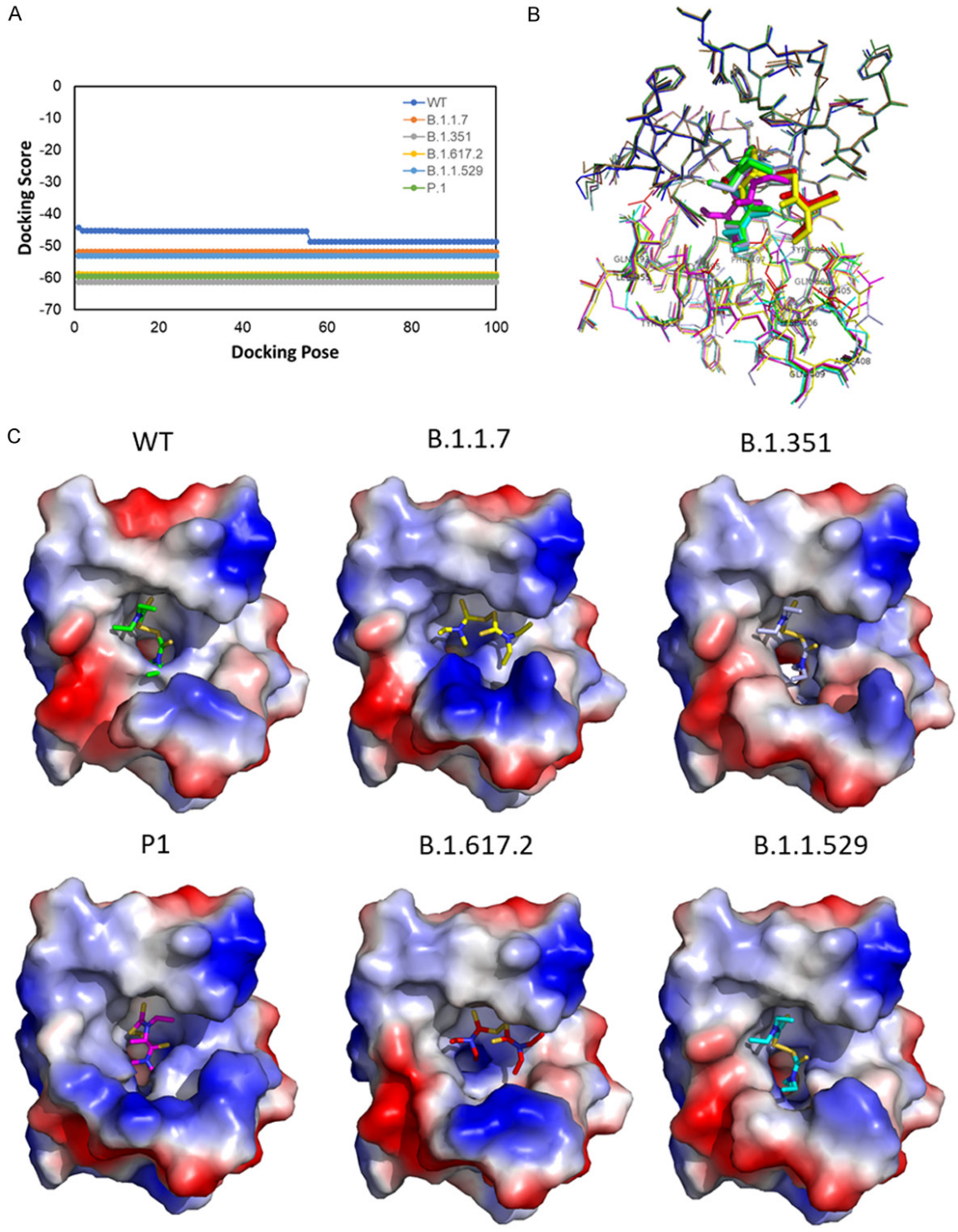

Figure 4. Conformation and pose of molecular docking interaction of disulfiram in the binding pocket of SARS-CoV-2_RDB-hACE2 complex. A. Disulfiram docking analysis for wild type and five variants of SARS-CoV-2. One hundred docking poses of disulfiram were analyzed for the targets of wild type (WT) and B.1.1.7 variant of SARS-CoV-2_RDB-hACE2 complex. The stability of docking disulfiram to wild-type and five variants are shown. B. The light colors represent SARS-CoV-2_RDB residues, whereas dark colors represent human ACE2. The green, yellow, red, light blue, magenta and cyan lines indicate residues of wild-type, B.1.1.7, B.1.1.529, B.1.351, B.1.617.2 and P1 variants, respectively. All the RDB residues are labeled. C. The contact potential of the binding pockets of WT and five variants with disulfiram. The red, blue, and white colors represent negative, positive, and hydrophobic areas, respectively.

proteins, supporting the results shown in **Figures 2** and **3** that disulfiram is able to inhibit viral entry.

Discussion

A vast amount of effort has been forged on developing vaccines to circumvent the SARS-CoV-2 pandemic. It is undeniable that vaccines are potent means to quell the pandemic; however, it is not clear whether vaccines alone can provide full immunity as new variants emerge. Due to the nature of viruses, they continue to evolve into new strains/variants that are better equipped at evading host protective immune systems [44]. Thus, the development of antiviral pharmacologic agents to treat COVID-19 should be warranted to minimize virus-caused severe symptoms in the host. New drug development is a challenging and expensive process. Repurposing old drugs could serve as an appealing, feasible strategy to lower costs and save time. Here, we report that disulfiram could be repurposed into a potent inhibitor of SARS-CoV-2 since we found that disulfiram can block spike protein binding to host receptor ACE2 to interrupt virus infection. We noticed that disulfiram was able to block live viral entry with similar potency for the wild-type and B.1.617.2 variants. However, it has less effect on the inhibition of viral replication for the B.1.1.7 variant than wild-type virus. It has been documented that disulfiram can inhibit SARS-CoV-2 replication through several different mechanisms [25]. It is unclear how the B.1.1.7 variant is more resistant to disulfiram than the wild-type SARS-CoV-2 virus for viral replication. Since the mutant of the B.1.1.7 variant occurs in the spike protein, it is interesting to entertain that spike protein may have a role in the viral replication. For instance, it raises an interesting question, whether the slight difference in the docked pose of disulfiram with wild-type and different spike mutants (Supplementary Figure 5) might affect the interaction of disulfiram with critical enzymes for viral replication.

The trending of current therapy is targeting more than one disease pathway, including combinations of two or more different treatments or therapeutics [45]. However, clinical development is time-consuming and expensive to determine and optimize the best combinations [46]. Because SARS-CoV-2 is an RNA coronavirus that typically has higher mutation rates, many variants of SARS-CoV-2 have been found and caused multiple waves [47]. An anti-viral drug with only one target, such as M^{pro} or the spike protein, might more easily cause resistance. Molecules with dual or multiple inhibitory activities against two or more different kinds of diseases would be ideal [33, 48, 49]. Ideally, one could identify existing compounds that are in use in clinics to stop or substantially diminish both viral entry and viral replication. In that case, such dual or multiple inhibitions may enhance the potency of these compounds in treating the coronavirus infection. Several other studies [25, 26, 28] have indicated that disulfiram could target multiple virus proteins involved in different processes of the viral life cycle, including transcription and replication. Here, we further demonstrated that disulfiram play a role for blocking viral entry. Remarkably, disulfiram is currently under evaluation in phase II clinical trials to treat COVID-19 (NCT04485130). A retrospective cohort study suggests that disulfiram contributes to the reduced incidence and severity of COVID-19 [50]. These results strongly support the clinical potential of disulfiram to treat COVID-19.

Acknowledgements

We would like to acknowledge the service provided by the Biosafety Level-3 Laboratory of the First Core Laboratory, National Taiwan University College of Medicine. We would also like to thank Tai-Ling Chao, Jun-Tung Fang, and Siman Ieong at National Taiwan University for their assistance with SARS-CoV-2 virus experiments. We thank the National RNAi Core Facility at Academia Sinica in Taiwan for providing all SARS-CoV-2 spike-pseudotyped lentiviruses and related services. We thank Dr. Jeng Cheng for editing this manuscript. This work was supported by grants from the Ministry of Science and Technology, Taiwan (MOST-109-2327-B-039-003, MOST-110-2740-B-002-006, MOST-109-2327-B-002-009 and MOST-110-2639-B-039-001-ASP).

Disclosure of conflict of interest

None.

Address correspondence to: Mien-Chie Hung, Drug Development Center, China Medical University, 100, Sec. 1, Jingmao Road, Beitun District, Taichung 406040, Taiwan. Tel: +886-04-22057153; Fax: +886-04-22952121; E-mail: mhung@cmu.edu.tw

References

[1] Banys P. The clinical use of disulfiram (Antabuse): a review. J Psychoactive Drugs 1988; 20: 243-261.

[2] Bell RG and Smith HW. Preliminary report on clinical trials of antabuse. Can Med Assoc J 1949; 60: 286-288.

[3] Koppaka V, Thompson DC, Chen Y, Ellermann M, Nicolaou KC, Juvonen RO, Petersen D, Deitrich RA, Hurley TD and Vasiliou V. Aldehyde dehydrogenase inhibitors: a comprehensive review of the pharmacology, mechanism of action, substrate specificity, and clinical application. Pharmacol Rev 2012; 64: 520-539.

[4] Schirmer HK and Scott WW. Disulfiram and tumor inhibition. Trans Am Assoc Genitourin Surg 1966; 58: 63-66.

[5] Lu C, Li X, Ren Y and Zhang X. Disulfiram: a novel repurposed drug for cancer therapy. Cancer Chemother Pharmacol 2021; 87: 159-172.

[6] Cen D, Brayton D, Shahandeh B, Meyskens FL Jr and Farmer PJ. Disulfiram facilitates intracellular Cu uptake and induces apoptosis in human melanoma cells. J Med Chem 2004; 47: 6914-6920.

[7] Chen D, Cui QC, Yang H and Dou QP. Disulfiram, a clinically used anti-alcoholism drug and copper-binding agent, induces apoptotic cell death in breast cancer cultures and xenografts via inhibition of the proteasome activity. Cancer Res 2006; 66: 10425-10433.

[8] Nobel CI, Kimland M, Lind B, Orrenius S and Slater AF. Dithiocarbamates induce apoptosis in thymocytes by raising the intracellular level of redox-active copper. J Biol Chem 1995; 270: 26202-26208.

[9] Yip NC, Fombon IS, Liu P, Brown S, Kannappan V, Armesilla AL, Xu B, Cassidy J, Darling JL and Wang W. Disulfiram modulated ROS-MAPK and NFkappaB pathways and targeted breast cancer cells with cancer stem cell-like properties. Br J Cancer 2011; 104: 1564-1574.

[10] Yang S, Yang L, Li X, Li B, Li Y, Zhang X, Ma Y, Peng X, Jin H and Li H. New insights into autophagy in hepatocellular carcinoma: mechanisms and therapeutic strategies. Am J Cancer Res 2019; 9: 1329-1353.

[11] Zhou B, Guo L, Zhang B, Liu S, Zhang K, Yan J, Zhang W, Yu M, Chen Z, Xu Y, Xiao Y, Zhou J, Fan J, Li H and Ye Q. Disulfiram combined with copper induces immunosuppression via PD-L1 stabilization in hepatocellular carcinoma. Am J Cancer Res 2019; 9: 2442-2455.

[12] Jiao Y, Hannafon BN and Ding WQ. Disulfiram's anticancer activity: evidence and mechanisms. Anticancer Agents Med Chem 2016; 16: 1378-1384.

[13] McMahon A, Chen W and Li F. Old wine in new bottles: advanced drug delivery systems for disulfiram-based cancer therapy. J Control Release 2020; 319: 352-359.

[14] Horita Y, Takii T, Yagi T, Ogawa K, Fujiwara N, Inagaki E, Kremer L, Sato Y, Kuroishi R, Lee Y, Makino T, Mizukami H, Hasegawa T, Yamamoto R and Onozaki K. Antitubercular activity of disulfiram, an antialcoholism drug, against multidrug- and extensively drug-resistant Mycobacterium tuberculosis isolates. Antimicrob Agents Chemother 2012; 56: 4140-4145.

[15] Long TE. Repurposing thiram and disulfiram as antibacterial agents for multidrug-resistant staphylococcus aureus infections. Antimicrob Agents Chemother 2017; 61: e00898-17.

[16] Galkin A, Kulakova L, Lim K, Chen CZ, Zheng W, Turko IV and Herzberg O. Structural basis for inactivation of Giardia lamblia carbamate kinase by disulfiram. J Biol Chem 2014; 289: 10502-10509.

[17] Shirley DA, Sharma I, Warren CA and Moonah S. Drug repurposing of the alcohol abuse medication disulfiram as an anti-parasitic agent. Front Cell Infect Microbiol 2021; 11: 633194.

[18] Elliott JH, McMahon JH, Chang CC, Lee SA, Hartogensis W, Bumpus N, Savic R, Roney J, Hoh R, Solomon A, Piatak M, Gorelick RJ, Lifson J, Bacchetti P, Deeks SG and Lewin SR. Short-term administration of disulfiram for reversal of latent HIV infection: a phase 2 dose-escalation study. Lancet HIV 2015; 2: e520-529.

[19] Lee SA, Elliott JH, McMahon J, Hartogenesis W, Bumpus NN, Lifson JD, Gorelick RJ, Bacchetti P, Deeks SG, Lewin SR and Savic RM. Population pharmacokinetics and pharmacodynamics of disulfiram on inducing latent HIV-1 transcription in a phase IIb trial. Clin Pharmacol Ther 2019; 105: 692-702.

[20] Lee YM, Duh Y, Wang ST, Lai MM, Yuan HS and Lim C. Using an old drug to target a new drug site: application of disulfiram to target the zn-site in HCV NS5A protein. J Am Chem Soc 2016; 138: 3856-3862.

[21] Lin MH, Moses DC, Hsieh CH, Cheng SC, Chen YH, Sun CY and Chou CY. Disulfiram can inhibit MERS and SARS coronavirus papain-like proteases via different modes. Antiviral Res 2018; 150: 155-163.

[22] Poduri R, Joshi G and Jagadeesh G. Drugs targeting various stages of the SARS-CoV-2 life cycle: exploring promising drugs for the treatment of Covid-19. Cell Signal 2020; 74: 109721.

[23] V'Kovski P, Kratzel A, Steiner S, Stalder H and Thiel V. Coronavirus biology and replication: implications for SARS-CoV-2. Nat Rev Microbiol 2021; 19: 155-170.

[24] Jin Z, Du X, Xu Y, Deng Y, Liu M, Zhao Y, Zhang B, Li X, Zhang L, Peng C, Duan Y, Yu J, Wang L, Yang K, Liu F, Jiang R, Yang X, You T, Liu X, Yang X, Bai F, Liu H, Liu X, Guddat LW, Xu W, Xiao G, Qin C, Shi Z, Jiang H, Rao Z and Yang H. Structure of M(pro) from SARS-CoV-2 and discovery of its inhibitors. Nature 2020; 582: 289-293.

[25] Sargsyan K, Lin CC, Chen T, Grauffel C, Chen YP, Yang WZ, Yuan HS and Lim C. Multi-targeting of functional cysteines in multiple conserved SARS-CoV-2 domains by clinically safe Zn-ejectors. Chem Sci 2020; 11: 9904-9909.

[26] Chen T, Fei CY, Chen YP, Sargsyan K, Chang CP, Yuan HS and Lim C. Synergistic inhibition of SARS-CoV-2 replication using disulfiram/Ebselen and remdesivir. ACS Pharmacol Transl Sci 2021; 4: 898-907.

[27] Sanyaolu A, Okorie C, Marinkovic A, Haider N, Abbasi AF, Jaferi U, Prakash S and Balendra V. The emerging SARS-CoV-2 variants of concern. Ther Adv Infect Dis 2021; 8: 20499361211024372.

[28] Wang YC, Yang WH, Yang CS, Hou MH, Tsai CL, Chou YZ, Hung MC and Chen Y. Structural basis of SARS-CoV-2 main protease inhibition by a broad-spectrum anti-coronaviral drug. Am J Cancer Res 2020; 10: 2535-2545.

[29] ChenY, Huang WC, Yang CS, Cheng FJ, Chiu YF, Chen HF, Huynh TK, Huang CF, Chen CH, Wang HC and Hung MC. Screening strategy of TMPRSS2 inhibitors by FRET-based enzymatic activity for TMPRSS2-based cancer and COVID-19 treatment. Am J Cancer Res 2021; 11: 827-836.

[30] Tuszynska I, Magnus M, Jonak K, Dawson W and Bujnicki JM. NPDock: a web server for protein-nucleic acid docking. Nucleic Acids Res 2015; 43: W425-430.

[31] Huang TT, Hwang JK, Chen CH, Chu CS, Lee CW and Chen CC. (PS)2: protein structure prediction server version 3.0. Nucleic Acids Res 2015; 43: W338-342.

[32] Hsu KC, Chen YF, Lin SR and Yang JM. iGEMDOCK: a graphical environment of enhancing GEMDOCK using pharmacological interactions and post-screening analysis. BMC Bioinformatics 2011; 12 Suppl 1: S33.

[33] Wang SC, Chen Y, Wang YC, Wang WJ, Yang CS, Tsai CL, Hou MH, Chen HF, Shen YC and Hung MC. Tannic acid suppresses SARS-CoV-2 as a dual inhibitor of the viral main protease and the cellular TMPRSS2 protease. Am J Cancer Res 2020; 10: 4538-4546.

[34] Shang J, Wan Y, Luo C, Ye G, Geng Q, Auerbach A and Li F. Cell entry mechanisms of SARS-CoV-2. Proc Natl Acad Sci U S A 2020; 117: 11727-11734.

[35] Matsuyama S, Nao N, Shirato K, Kawase M, Saito S, Takayama I, Nagata N, Sekizuka T, Katoh H, Kato F, Sakata M, Tahara M, Kutsuna S, Ohmagari N, Kuroda M, Suzuki T, Kageyama T and Takeda M. Enhanced isolation of SARS-CoV-2 by TMPRSS2-expressing cells. Proc Natl Acad Sci U S A 2020; 117: 7001-7003.

[36] Hoffmann M, Kleine-Weber H, Schroeder S, Kruger N, Herrler T, Erichsen S, Schiergens TS, Herrler G, Wu NH, Nitsche A, Müller MA, Drosten C and Pöhlmann S. SARS-CoV-2 cell entry depends on ACE2 and TMPRSS2 and is blocked by a clinically proven protease inhibitor. Cell 2020; 181: 271-280, e278.

[37] Izaguirre G. The proteolytic regulation of virus cell entry by furin and other proprotein convertases. Viruses 2019; 11: 837.

[38] Coutard B, Valle C, de Lamballerie X, Canard B, Seidah NG and Decroly E. The spike glycoprotein of the new coronavirus 2019-nCoV contains a furin-like cleavage site absent in CoV of the same clade. Antiviral Res 2020; 176: 104742.

[39] Indrayanto G, Putra GS and Suhud F. Validation of in-vitro bioassay methods: application in herbal drug research. Profiles Drug Subst Excip Relat Methodol 2021; 46: 273-307.

[40] Pena-Moran OA, Villarreal ML, Alvarez-Berber L, Meneses-Acosta A and Rodriguez-Lopez V. Cytotoxicity, post-treatment recovery, and selectivity analysis of naturally occurring podophyllotoxins from bursera fagaroides var. fagaroides on breast cancer cell lines. Molecules 2016; 21: 1013.

[41] Grabowski F, Preibisch G, Gizinski S, Kochanczyk M and Lipniacki T. SARS-CoV-2 variant of concern 202012/01 has about twofold replicative advantage and acquires concerning mutations. Viruses 2021; 13: 392.

[42] Touret F, Luciani L, Baronti C, Cochin M, Driouich JS, Gilles M, Thirion L, Nougairede A and de Lamballerie X. Replicative fitness of a SARS-CoV-2 20I/501Y.V1 variant from lineage B.1.1.7 in human reconstituted bronchial epithelium. mBio 2021; 12: e0085021.

[43] Vangone A, Schaarschmidt J, Koukos P, Geng C, Citro N, Trellet ME, Xue LC and Bonvin A. Large-scale prediction of binding affinity in protein-small ligand complexes: the PRODIGY-LIG web server. Bioinformatics 2019; 35: 1585-1587.

[44] McCarthy KR, Rennick LJ, Nambulli S, Robinson-McCarthy LR, Bain WG, Haidar G and Duprex WP. Recurrent deletions in the SARS-CoV-2 spike glycoprotein drive antibody escape. Science 2021; 371: 1139-1142.

[45] Bang S, Son S, Kim S and Shin H. Disease pathway cut for multi-target drugs. BMC Bioinformatics 2019; 20: 74.

[46] Kaur G. Polypharmacy: the past, present and the future. J Adv Pharm Technol Res 2013; 4: 224-225.
[47] Akkiz H. Implications of the novel mutations in the SARS-CoV-2 genome for transmission, disease severity, and the vaccine development. Front Med (Lausanne) 2021; 8: 636532.
[48] Zhou J, Jiang X, He S, Jiang H, Feng F, Liu W, Qu W and Sun H. Rational design of multitarget-directed ligands: strategies and emerging paradigms. J Med Chem 2019; 62: 8881-8914.
[49] Chen Y, Yang WH, Chen HF, Huang LM, Gao JY, Lin CW, Wang YC, Yang CS, Liu YL, Hou MH, Tsai CL, Chou YZ, Huang BY, Hung CF, Hung YL, Wang WJ, Su WC, Kumar V, Wu YC, Chao SW, Chang CS, Chen JS, Chiang YP, Cho DY, Jeng LB, Tsai CH and Hung MC. Tafenoquine and its derivatives as inhibitors for the severe acute respiratory syndrome coronavirus 2. J Biol Chem 2022; 298: 101658.
[50] Tamburin S, Mantovani E, De Bernardis E, Zipeto D and Lugoboni F; Gruppo InterSERT di Collaborazione Scientifica (GICS). COVID-19 and related symptoms in patients under disulfiram for alcohol use disorder. Intern Emerg Med 2021; 16: 1729-1731.

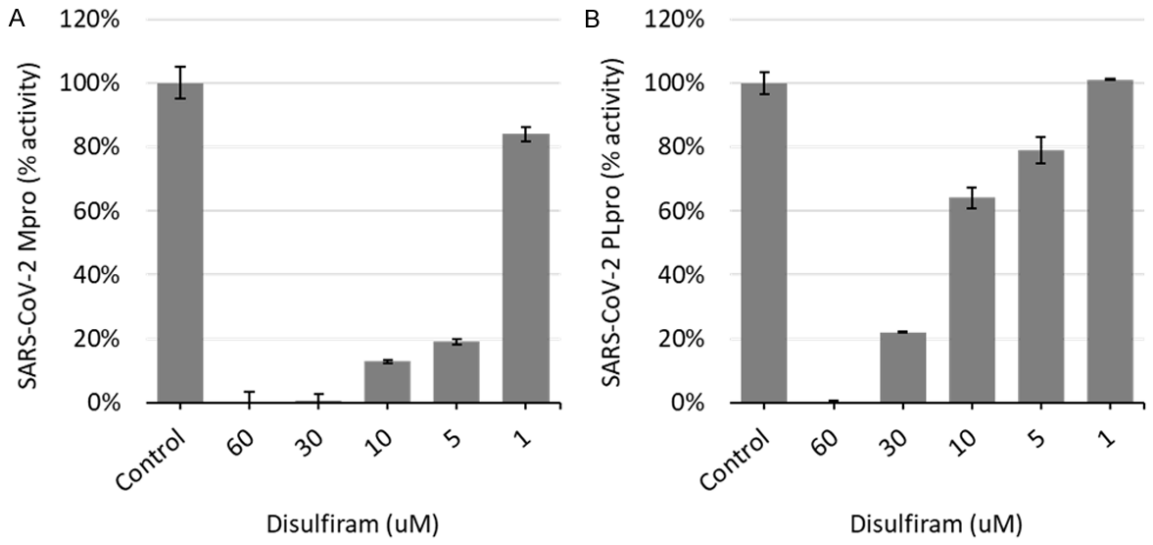

Supplementary Figure 1. Disulfiram inhibited the enzymatic activity of M^{pro} and PL^{pro}. A. The M^{pro} enzymatic activity was measured by using a FRET-base assay with the indicated concentration of disulfiram. B. The PL^{pro} enzymatic activity was measured by using a FRET-base assay with the indicated concentration of disulfiram. All data are shown as mean ± SD (n=3).

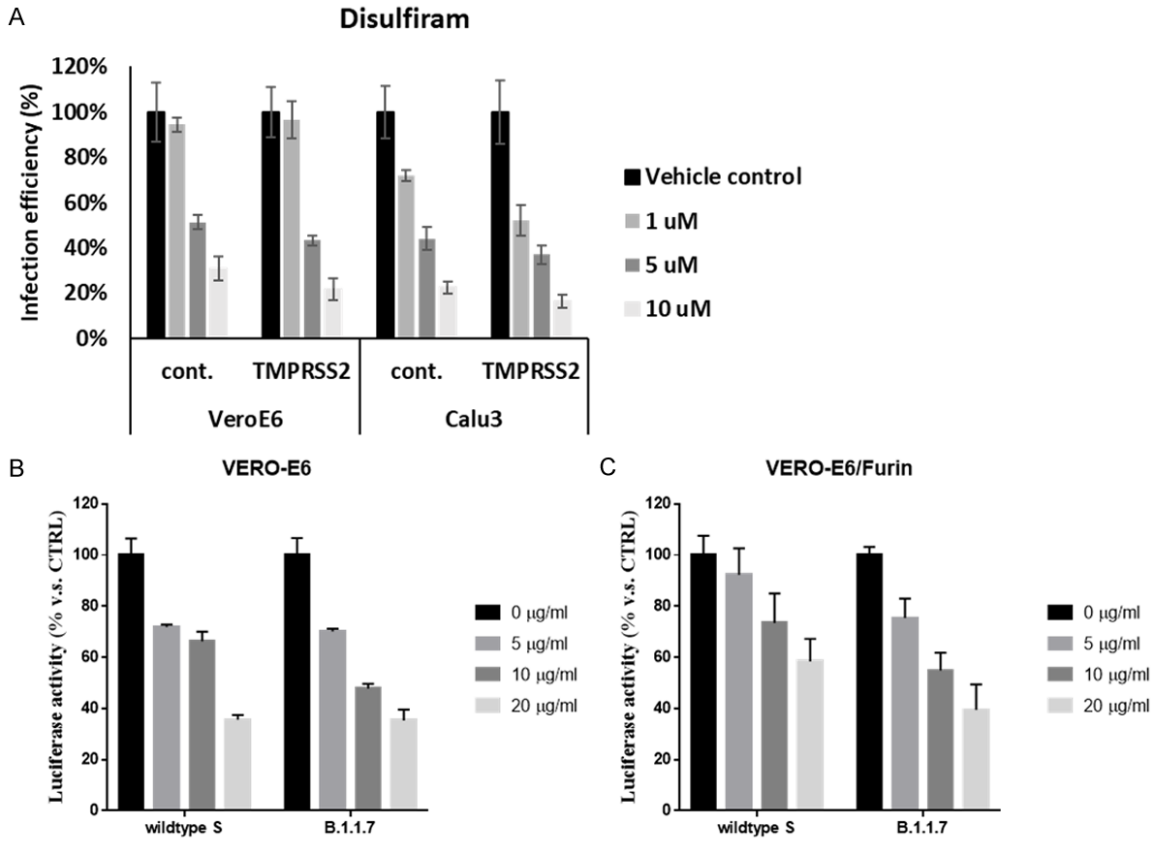

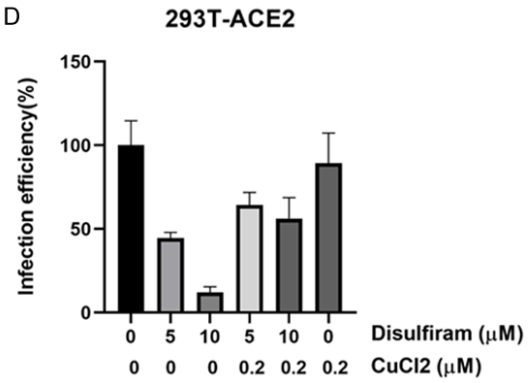

Supplementary Figure 2. Disulfiram inhibited SARS-CoV-2 spike vpp infection in different cell models. A. VeroE6 and Calu3 cells with and without TMPRSS2 over-expression were pretreated with the indicated concentrations of disulfiram and then infected with SARS-CoV-2 wild-type Spike vpps. After 24 hours of infection, the infection efficiency rate was measured according to luciferase activities. B. and C. The infection efficiency of VeroE6 or VeroE6/furin cells, which were pretreated with disulfiram and then infected with SARS-CoV-2 wild-type spike vpps, was shown. D. The infection efficiency of different combination treatments with disulfiram and $CuCl_2$ in 293T-ACE2 was evaluated. All data are shown as mean ± SD (n=3).

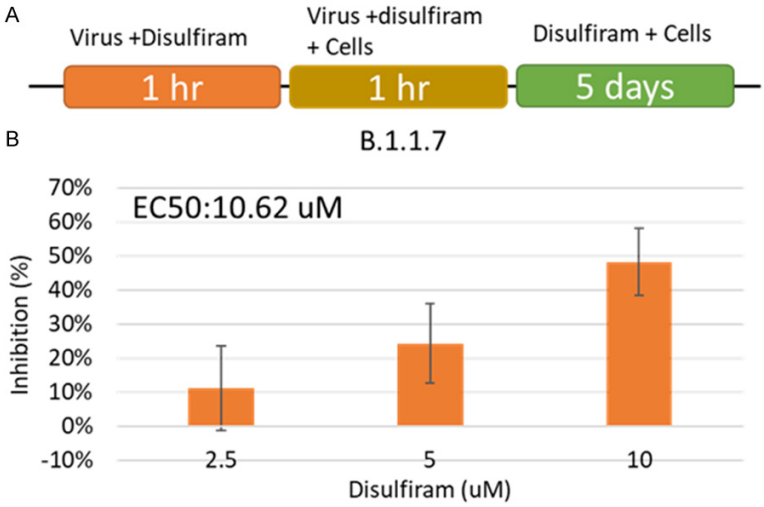

Supplementary Figure 3. Disulfiram inhibited virus infection of SARS-CoV-2 B.1.1.7 variants. A. Schematic illustrating method of B.1.1.7 variants live virus infection assay was shown. As depicted, VeroE6 cells were treated with disulfiram and B.1.1.7 variants and then collected for plaque assay after 5 days. B. The inhibition of different concentrations of disulfiram against B.1.1.7 variants in plaque formation results represents three independent experiments, each in triplicate. All data are shown as mean ± SD (N=3). The EC50 was determined using GraphPad PRISM software.

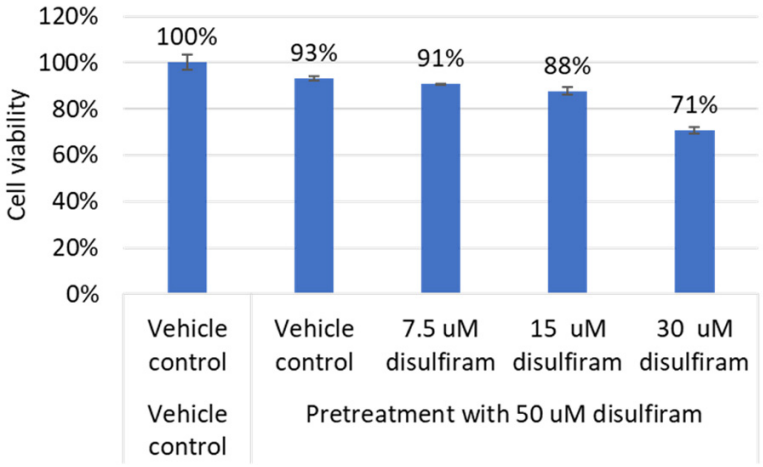

Supplementary Figure 4. In the pre-treatment model, disulfiram could not cause high toxicity. VeroE6 cells were pretreated vehicle control (DMSO) or 50 μM disulfiram for 1 hour and wash away, then treated with indicated concentrations of disulfiram. The cell viability was detected by MTT assay (N=3).

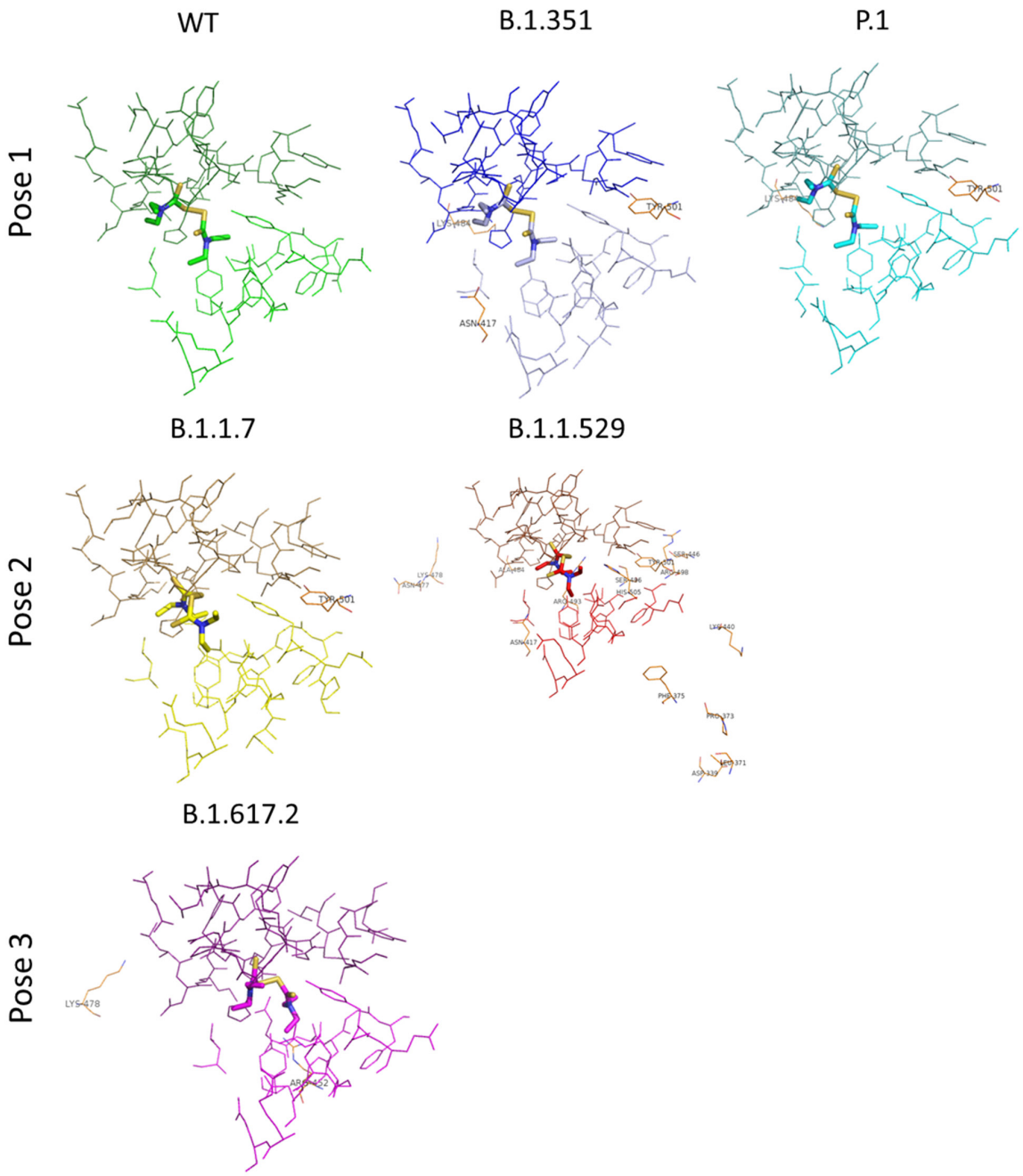

Supplementary Figure 5. The binding poses of disulfiram docked with the binding pocket of SARS-CoV-2_RDB-hACE2 for different SARS-CoV-2 variants. The poses of disulfiram docked to WT and 5 variants were shown. Pose 1 consisted of WT, B.1.351 and P1 variants. B.1.1.7 and B.1.1.529 variants belonged to Pose 2. Only B.1.617.2 was Pose 3. The RBD mutations revealed in each variant are shown in orang lines with labels.